DNA Condensation by Polyamines: A Laser Light Scattering Study of Structural Effects†

Veena Vijayanathan,‡ Thresia Thomas,§,||,⊥ Akira Shirahata,# and T. J. Thomas*,‡,⊥

Department of Medicine, Department of Environmental and Community Medicine, The Environmental and Occupational Health Sciences Institute, and The Cancer Institute of New Jersey, University of Medicine and Dentistry of New Jersey−Robert Wood Johnson Medical School, New Brunswick, New Jersey 08903, and Department of Biochemistry, Faculty of Pharmaceutical Sciences, Josai University, Sakado, Saitama 350-02, Japan

Received May 15, 2001; Revised Manuscript Received August 7, 2001

ABSTRACT: Polyamines such as spermidine and spermine are abundant in living cells and are believed to aid in the dense packaging of cellular DNA. DNA condensation is a prerequisite for the transport of gene vectors in living cells. To elucidate the structural features of polyamines governing DNA condensation, we studied the collapse of λ-DNA by spermine and a series of its homologues, $H_2N(CH_2)_3NH(CH_2)_{n=2-12}NH(CH_2)_3NH_2$ ($n = 4$ for spermine), using static and dynamic light scattering techniques. All polyamines provoked DNA condensation; however, their efficacy varied with the structural geometry of the polyamine. In 10 mM sodium cacodylate buffer, the EC_{50} values for DNA condensation were comparable (4 ± 1 μM) for spermine homologues with $n = 4-8$, whereas the lower and higher homologues provoked DNA condensation at higher EC_{50} values. The EC_{50} values increased with an increase in the monovalent ion (Na^+) concentration in the buffer. The slope of a plot of log [EC_{50}(polyamine^{4+})] against log [Na^+] was ~1.5 for polyamines with even number values of *n*, whereas the slope value was ~1 for compounds with odd number values of *n*. Dynamic light scattering measurements showed the presence of compact particles with hydrodynamic radii (R_h) of about 40−50 nm for compounds with $n = 3-6$. R_h increased with further increase in methylene chain length separating the secondary amino groups of the polyamines ($R_h = 60-70$ nm for $n = 7-10$ and >100 nm for $n = 11$ and 12). Determination of the relative binding affinity of polyamines to DNA using an ethidium bromide displacement assay showed that homologues with $n = 2$ and 3 as well as those with $n > 7$ had significantly lower DNA binding affinity compared to spermine and homologues with $n = 5$ and 6. These data suggest that the chemical structure of isovalent polyamines exerts a profound influence on their ability to recognize and condense DNA, and on the size of the DNA condensates formed in aqueous solution.

DNA condensation into compact structures has received considerable attention in recent years due to its biological implications in DNA packaging in virus heads and chromatin as well as to understand the mechanism of uptake of gene vectors in living cells (*1*−*5*). Several studies have demonstrated the efficacy of internal proteins, neutral polymers, and polyamines in condensing DNA (*6*−*13*). The relative effectiveness of various cations in condensing DNA generally depends on valence, those with higher positive charge inducing condensation at lower concentrations (*8*). Compaction of DNA is favored when 89−90% of the negative charge density of DNA is neutralized by multivalent cations. Linear cellular cations such as the ubiquitous polyamines, spermidine and spermine, aid in the packaging of cellular DNA in a compact state by lowering the free energy of transition (*14*). Among the naturally occurring polyamines, spermine is more efficacious in stabilizing and condensing DNA than putrescine and spermidine (*8*). In vitro, these polycations neutralize the DNA phosphate charge and provoke monomolecular condensation into compact forms such as rods, toroids, and spheroids, which are structurally similar to phage DNA in the precursor capsid of viruses (*10, 12, 15*−*18*).

Polyamine-mediated DNA condensation belongs to the more general class of cation-induced DNA condensation (*1*−*4*). In this process, DNA is in the B form, and condensation is intramolecular at low concentrations, with condensates having a toroidal appearance in the electron and atomic force microscope (*18, 19*). Studies by Wilson and Bloomfield (*8*) on polyamine-induced condensation of T7 DNA by total intensity and quasi-elastic laser light scattering showed that

† This work was supported by U.S. Public Health Service Grants CA80163, CA42439, and CA73058 (to T.J.T. and T.T.) and by a Grant-in-Aid for Scientific Research from the Ministry of Education, Science and Culture, Japan (to A.S.).

* Correspondence should be addressed to this author at 125 Paterson St., Clinical Academic Building, Room 7090, New Brunswick, NJ 08903. Phone: (732) 235-8460. Fax: (732) 235-8473. E-mail: thomastj@umdnj.edu.

‡ Department of Medicine, University of Medicine and Dentistry of New Jersey−Robert Wood Johnson Medical School.

§ Department of Environmental and Community Medicine, University of Medicine and Dentistry of New Jersey−Robert Wood Johnson Medical School.

|| The Environmental and Occupational Health Sciences Institute, University of Medicine and Dentistry of New Jersey−Robert Wood Johnson Medical School.

⊥ The Cancer Institute of New Jersey, University of Medicine and Dentistry of New Jersey−Robert Wood Johnson Medical School.

Department of Biochemistry, Josai University.

10.1021/bi010993t CCC: $20.00
Published on Web 10/13/2001

the amount of polyamines required to induce the condensation process varied by more than 3 orders of magnitude over a range of Na^+ and Mg^{2+} concentrations. These authors successfully applied the counterion condensation theory, developed by Manning (*20*) and Record et al. (*21*), to calculate the polyelectrolyte charge neutralization during the collapse of DNA by polyamines. Binding studies of polyamines to DNA using equilibrium dialysis (*22*) as well as NMR (*23*) and Raman spectroscopy (*24*) indicated nonspecific, electrostatic interactions between DNA phosphates and polyamines. However, X-ray crystallographic analysis (*25*−*28*) and molecular modeling (*29*) suggested that polyamines might occupy specific sites, especially the major and minor grooves, in different DNA conformations. Polyamine structural specificity effects appear to play an important role in the induction and stabilization of left-handed Z-DNA and triplex DNA also (*30, 31*).

Thomas and Bloomfield (*10*) investigated the ability of two trivalent cations, $Co(NH_3)_6^{3+}$ and spermidine^{3+}, to condense T7 DNA and found significant differences in the critical concentrations of these cations to provoke the condensation process. The size of the condensates was generally smaller with $Co(NH_3)_6^{3+}$ compared to that of spermidine^{3+}, as measured by dynamic laser light scattering. Allison et al. (*32*) further found differences in the ability of a series of spermidine homologues to induce the condensation of φ29 phage DNA. Srivenugopal et al. (*33*) reported that the concentration of spermidine homologues necessary to aggregate negatively supercoiled Col E1 DNA progressively increased as the diaminobutane moiety of spermidine was extended beyond five methylene groups. Schellman and Parthsarathy (*34*) showed that the structural arrangement of DNA precipitated by the spermidine homologues had a strong dependence on the chemical structure of the polyamines. The Bragg spacing and the calculated interhelical spacing for a hexagonal packing model of DNA varied systematically with the length of the methylene bridge. Recent studies further show significant differences in the ability of a group of spermine analogues to aggregate oligonucleotides and genomic DNA (*35*). However, the structural specificity effect of tetravalent spermine homologues on DNA condensation has not yet been investigated.

To understand the role of polyamine structure in DNA condensation, we synthesized a series of spermine homologues, $H_2N(CH_2)_3NH(CH_2)_{n=2-12}NH(CH_2)_3NH_2$ ($n = 4$ for spermine) and studied their ability to condense λ-DNA by total intensity and quasi-elastic laser light scattering techniques and found a marked effect of the length of the central methylene region of polyamines on their ability to induce the condensation and the R_h[1] of the condensates formed.

MATERIALS AND METHODS

DNAs. Highly purified λ-phage DNA was purchased from Sigma Chemical Co. (St. Louis, MO). This DNA was dissolved in 10 mM cacodylate buffer (10 mM sodium cacodylate, pH 7.2, and 0.5 mM EDTA) and was extensively dialyzed against the same buffer. The concentration of the stock solution was adjusted to 1 mg/mL. The absorbance ratio (A_{260}/A_{280}) was 1.9, indicating that the DNA was free of protein contamination. The stock DNA solution was further diluted in 10 mM cacodylate buffer to give a concentration of 0.5 μg/mL.

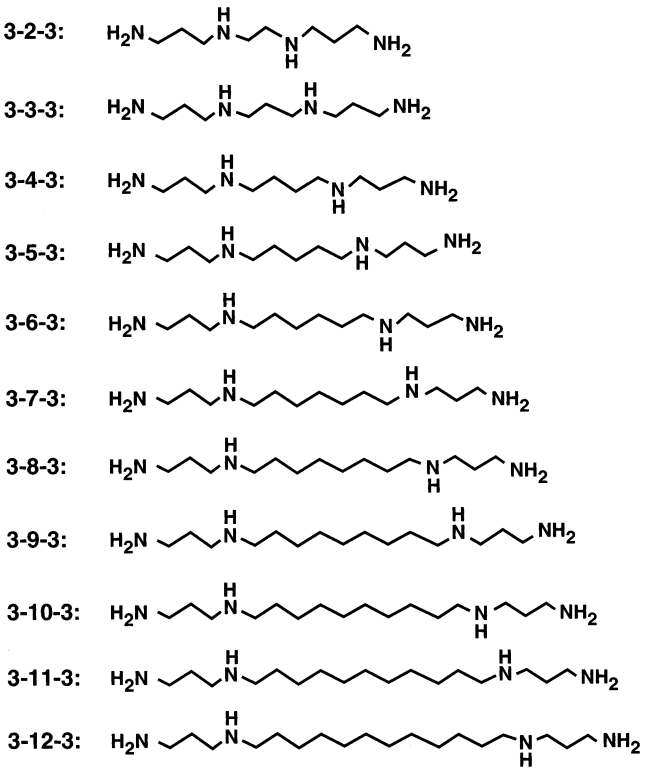

FIGURE 1: Chemical structures of spermine and its homologues used in this study.

Polyamines and Reagents. Spermine·4HCl was purchased from Sigma Chemical Co. The structural homologues of spermine, 1,10-diamino-4,7-diazadecane (3-2-3), 1,11-diamino-4,8-diazaundecane (3-3-3), 1,13-diamino-4,10-diazatridecane (3-5-3), 1,14-diamino-4,11-diazatetradecane (3-6-3), 1,15-diamino-4,12-diazapentadecane (3-7-3), 1,16-diamino-4,13-diazahexadecane (3-8-3), 1,17-diamino-4,14-diazaheptadecane (3-9-3), 1,18-diamino-4,15-diazanonadecane (3-10-3), 1,19-diamino-4,16-diazaeicosane (3-11-3), and 1,20-diamino-4,17-diazaheneicosane (3-12-3), were synthesized as described previously (*36, 37*). The structure and purity of all polyamine homologues were confirmed by elemental analysis, NMR, HPLC, and mass spectrometry. The chemical structures of these polyamine homologues are given in Figure 1. Polyamine homologue stock solutions (50 mM) were prepared in sterile, double-distilled water, and appropriate dilutions were made in 10 mM cacodylate buffer.

All other reagents, including ethidium bromide and chemicals for buffers, were of the highest purity and purchased from Sigma Chemical Co.

Total Intensity Light Scattering. Light scattering experiments were performed using a Fluoromax-2 spectrofluorometer (Jobin Yvon-Spex Instruments S. A., Inc., Edison, NJ). Light from a 150 W xenon lamp was filtered through double monochromators. The excitation and emission monochromators were set to the same wavelength of 305 nm with 5

[1] Abbreviations: R_h, hydrodynamic radius; 3-2-3, 1,10-diamino-4,7-diazadecane; 3-3-3, 1,11-diamino-4,8-diazaundecane; 3-5-3, 1,13-diamino-4,10-diazatridecane; 3-6-3, 1,14-diamino-4,11-diazatetradecane; 3-7-3, 1,15-diamino-4,12-diazapentadecane; 3-8-3, 1,16-diamino-4,13-diazahexadecane; 3-9-3, 1,17-diamino-4,14-diazaheptadecane; 3-10-3, 1,18-diamino-4,15-diazanonadecane; 3-11-3, 1,19-diamino-4,16-diazaeicosane; 3-12-3, 1,20-diamino-4,17-diazaheneicosane.

nm band-pass, the integration time was set to 5 s to increase the sensitivity, and the scattered light intensity was collected at a 90° angle with respect to the incident beam. The condensation experiment was performed in 10 mM cacodylate buffer, pH 7.2. All buffers were filtered through 0.25 μm type GS Millipore filters before use. A concentration of 0.25−0.5 μg/mL DNA solution was used in a 2 mL disposable borosilicate glass tube. Small quantities (<10 μL) of polyamine solutions were added to the DNA solution to the desired concentration; the solution was mixed gently and kept undisturbed for a period of 30 min at 22 °C to attain equilibrium. The solution was then centrifuged at 500*g* for about 30 min at 22 °C using a Beckman GS 6KR centrifuge to reduce light scattering from dust and aggregate particles. To determine the effect of centrifugation on the concentration of DNA in the supernatant, we measured the A_{260} value of the solution before centrifugation and that of the supernatant after centrifugation. There was no reduction in the DNA concentration after centrifugation under the conditions of our experiment or even at 10-fold higher DNA concentrations. Therefore, centrifugation at 500*g* does not result in DNA phase separation, and hence the light scattering measurements are representative of the DNA concentrations used in our study.

Dynamic Laser Light Scattering. Dynamic laser light scattering experiments were conducted using a DynaPro model MSX (Protein Solutions, Inc., Charlottesville, VA) equipped with a 2 W laser and a wavelength of 800 nm. A laser beam was passed through a small quartz cell containing the sample (polyamine/DNA mixture), and the scattered light was detected at a 90° angle to the incident beam, and analyzed with an autocorrelator to generate and normalize the first-order autocorrelation function. For monodisperse particles much smaller than the incident beam, the autocorrelation function, $g^{(1)}(\tau)$, is given by the equation (*38*):

$$g^{(1)}(\tau) = \exp[-Dq^2(\tau)] \quad (1)$$

where τ is the decay time and q ($=4\pi n/[\lambda_0 \sin(\theta/2)]$) is the scattering vector which is a function of the solvent refractive index n, the wavelength of the incident beam λ_0, the scattering angle θ, and the diffusion coefficient D. The hydrodynamic radius (R_h) is calculated from the diffusion coefficient using the Stokes−Einstein equation:

$$R_h = kT/6\pi\eta D \quad (2)$$

where k is the Boltzmann constant, T is the absolute temperature, and η is the solvent viscosity.

Data analysis was performed using a Dynamics Version 6 software package supplied by the manufacturer (Protein Solutions, Inc.). Unimodal analysis was performed on each data set, and the autocorrelation function was treated as a single decaying exponential with a decay constant directly proportional to the diffusion coefficient of the sample. The quantitative goodness-of-fit between the measured and theoretical data, where a monomodal, narrow molecular weight distribution is assumed, is calculated by a cumulant method of analysis.

The correlation function of individual components is related to decay rate by the expression:

$$D_i q^2 = (kT/6\pi\eta R_i)[(2\pi n/\lambda_0) \sin(\theta/2)]^2 \quad (3)$$

where D_i and R_i, respectively, are the diffusion coefficient and hydrodynamic radius ($R = R_h$) of that component. The normalized display of the area under the curve for each exponential contribution (A_i) versus R is the percent intensity of the distribution of the histogram, and the mean radius of a particular subpeak is obtained from the histogram using the expression:

$$\langle R \rangle = \Sigma A_i R_i / \Sigma A_i \quad (4)$$

DNA solutions were prepared, mixed with polyamine solutions, and centrifuged to remove dust and aggregated particles, as described above for the total intensity light scattering experiment. Then 12 μL of the supernatant solution was transferred to the standard quartz cuvette, and the scattered light was measured at 22 °C at an angle of 90° to the incident beam. All measurements were performed in the same cuvette to avoid variations due to minor differences between cuvettes. The cuvette was washed, rinsed thoroughly with milliQ water, and dried before each measurement.

Ethidium Bromide Displacement Assay. The relative binding affinity of spermine homologues to λ-DNA was determined using the ethidium bromide displacement assay, as described previously (*39*, *40*). Binding of polyamines to DNA causes a displacement of bound ethidium bromide, resulting in a decrease in the fluorescence emission intensity. Aliquots of polyamines were sequentially added to a solution of DNA (2 μM) containing 1 μg/mL ethidium bromide in 10 mM cacodylate buffer at pH 7.2. After each addition, the mixture was carefully stirred and fluorescence emission intensity measured at 590 nm with an excitation wavelength of 510 nm. The total polyamine solution added to the DNA solution did not exceed 5% of the total volume of the solution, and hence no correction was made for sample dilution. All fluorescence measurements were made using a Fluoromax-2 spectrofluorometer.

RESULTS

Static Light Scattering. Figure 2 shows the relative intensity of scattered light from DNA solutions incubated with different concentrations of spermine and three of its higher homologues, 3-10-3, 3-11-3, and 3-12-3. The light scattering intensity of a dilute solution of DNA was low and remained unchanged at low concentrations of polyamines. However, at a critical concentration of the polyamines (4−20 μM, depending on the homologue), a rapid increase in the scattered light intensity occurred, which then leveled off to a plateau value, independent of further addition of polyamines. The increase in the intensity of the scattered light has been attributed to the compaction of DNA with a large increase in the surface area of the particulate state of the macromolecule. To quantify the efficacy of different polyamines in condensing DNA, we calculated the EC_{50} values, concentrations of polyamines at the midpoint of DNA condensation. Figure 3 shows the EC_{50} values of spermine and 10 of its homologues plotted against the number (n) of methylene groups bridging the secondary amino groups of the tetramines. The EC_{50} values of the lower homologues of spermine, 3-2-3 and 3-3-3, were ~2-fold higher than that of spermine. The EC_{50} values were comparable (4 ± 1 μM)

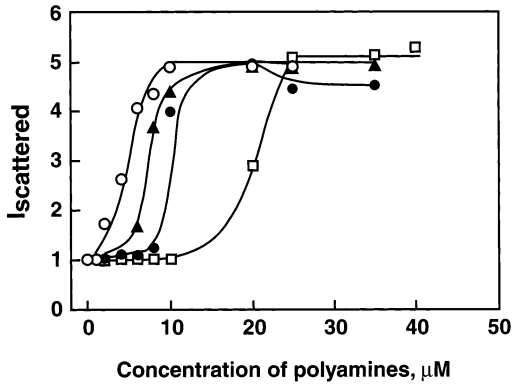

FIGURE 2: Typical plots of the relative intensity of scattered light at 90° plotted against the concentrations of spermine (○), 3-10-3 (▲), 3-11-3 (●), and 3-12-3 (□). The λ-DNA solution had a concentration of 1.5 μM DNA phosphate, dissolved in 10 mM sodium cacodylate buffer, pH 7.4.

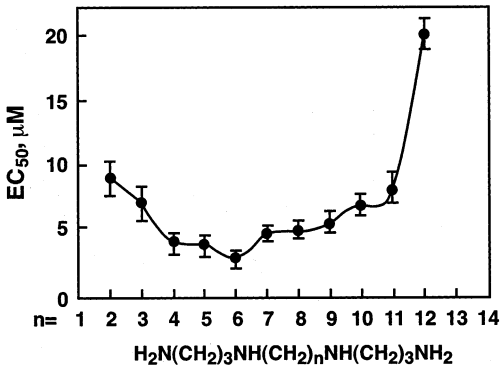

FIGURE 3: Polyamine structural effects on DNA condensation. The midpoint concentration (EC_{50}) of spermine homologues necessary to induce DNA condensation is plotted against the number of methylene groups between the secondary amino groups of spermine. Error bars indicate standard deviation from 3 separate experiments.

for spermine, 3-5-3, 3-6-3, 3-7-3, and 3-8-3, although 3-6-3 had the lowest EC_{50} value (2.9 ± 0.5 μM). However, there was an increase in the EC_{50} values with the higher homologues, 3-9-3, 3-10-3, 3-11-3, and 3-12-3, indicating that structural specificity effects might play an important role in the ability of these compounds in condensing λ-DNA.

Effect of Salt Concentration. We next determined the effect of ionic conditions of the medium on the efficacy of polyamines to condense λ-DNA by adjusting the monovalent salt concentration of the buffer using 1 M NaCl stock solution. The effect of salt concentration on the effectiveness of different polyamines to condense λ-DNA is given in Figure 4. As the concentration of Na^+ increased, the concentration of polyamines required for DNA condensation also increased, and straight lines were obtained on plotting log [EC_{50}] values against log [Na^+]. The slopes of these lines were between 0.9 and 1.6. This slope value, d log [EC_{50}]/d log[Na^+], is a quantitative measure of the concentration dependence between multivalent and monovalent cations in condensing DNA. Interestingly, there was a periodic oscillation of these slope values between odd and even number of methylene groups in the central region of the tetramine (Figure 5). However, 3-10-3 and 3-11-3 did not follow the same trend as that of the other homologues. This might be due to the ability of these molecules to enter intermolecular interactions, leading to cross-linking of several DNA molecules. The increased EC_{50} values of these higher homologues also indicate that their effectiveness as condensing agents is reduced by the fraction that enters into interhelical interactions (*30*).

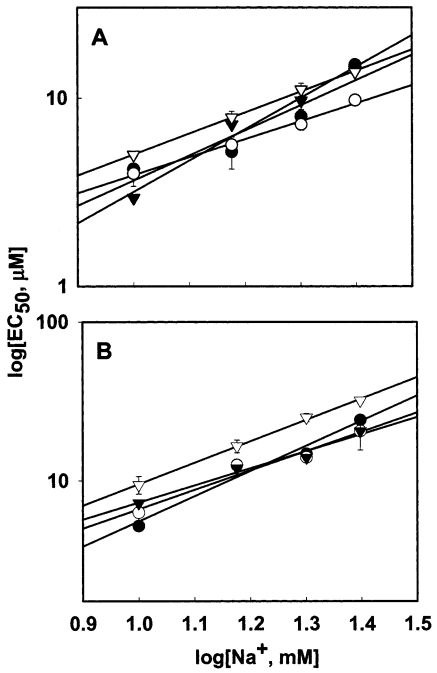

FIGURE 4: Effect of [Na^+] in the buffer on the midpoint concentration of polyamines (EC_{50}) to induce DNA condensation. The symbols represent EC_{50} values for (A): 3-4-3 (●), 3-5-3 (○), 3-6-3 (▼), and 3-7-3 (▽), and (B): 3-8-3 (●), 3-9-3 (○), 3-10-3 (▼), and 3-11-3 (▽). Error bars indicate standard deviation from 3 separate experiments.

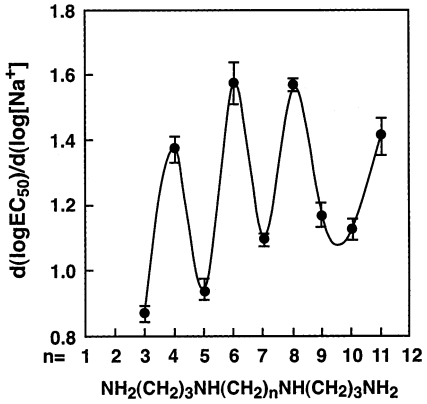

FIGURE 5: Plot of d (log [EC_{50}])/d (log [Na^+]) against the number of methylene groups on the central methylene core of spermine. Error bars indicate standard deviation from 3 separate experiments.

Measurement of Hydrodynamic Radii of DNA Condensates. We next determined the diffusion coefficients/hydrodynamic radii of DNA condensates formed in the presence of spermine and its homologues. Dynamic light scattering measurements indicated the presence of highly compacted DNA structures in the presence of spermine, with a diffusion coefficient of 5×10^{-8} cm^2/s, corresponding to a Stokes radius of 41 ± 5 nm. The data on diffusion coefficients and hydrodynamic radii are presented in Table 1. The histogram analysis showed a narrow range of hydrodynamic radii for DNA condensates formed in the presence of spermine and its homologues (Figure 6). The R_h values of spermine (3-4-3) and its nearest homologues (3-3-3, 3-5-3, and 3-6-3) were between 40 and 50 nm;

Table 1: Hydrodynamic Properties of DNA Condensates Formed in the Presence of Spermine and Its Homologues

polyamine homologue	diffusion coefficient (cm^2/s)	hydrodynamic radius[a] (nm)
3-3-3	4.5×10^{-8}	50
3-4-3 (spermine)	5.5×10^{-8}	41
3-5-3	4.7×10^{-8}	50
3-6-3	4.8×10^{-8}	48
3-7-3	4.0×10^{-8}	59
3-8-3	3.6×10^{-8}	63
3-9-3	3.4×10^{-8}	67
3-10-3	3.3×10^{-8}	69
3-11-3	2.4×10^{-8}	101
3-12-3	1.7×10^{-8}	132

[a] The reproducibility with these measurements was within 5% in repeated measurements.

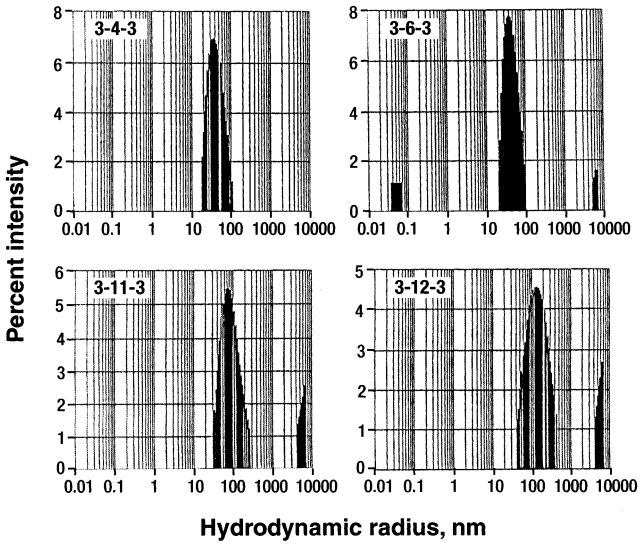

FIGURE 6: Histogram plots of the intensity of DNA condensates of different hydrodynamic radii against the hydrodynamic radius. All hydrodynamic measurements were done with dynamic light scattering equipment in 10 mM sodium cacodylate buffer. Histograms were generated using the Dynamic version 6 software, as described in the text.

however, the R_h values increased with the length of the methylene bridging region to 60−70 nm for 3-7-3, 3-8-3, 3-9-3, and 3-10-3, and to >100 nm for 3-11-3 and 3-12-3. The histogram for 3-12-3 also showed the presence of a small quantity of a larger species in the condensates, and small particles for 3-6-3 and 3-9-3. However, we did not observe any change in the size of the condensates when the concentration of DNA was increased from 0.25 to 0.5 μg/mL.

Relative Binding Affinity of Spermine Homologues for DNA. We also determined the relative binding affinities of spermine and its homologues with DNA using the fluorescence quenching assay, based upon the displacement of fluorescent ethidium bromide from DNA upon addition of polyamines (*39, 40*). Polyamines compete with ethidium for binding to DNA, and the concentration of polyamines required to quench the fluorescence of the ethidium bromide−DNA complex by 50% is inversely proportional to the binding constant. Thus, the relative binding constants were calculated, with spermine given the value of unity (Table 2). The relative binding affinity of the homologues increased from 3-2-3 to 3-5-3, and thereafter decreased with increase in the number of methylene groups in the central region of the tetramines. These results indicate that charge and hydrophobicity of the ligands might play a significant role in the binding affinity of the polyamines to DNA.

Table 2: Relative Binding Constants Measured by the Ethidium Competition Method

polyamine homologue	relative binding constant[a]
3-2-3	0.4
3-3-3	0.6
3-4-3 (spermine)	1.0
3-5-3	1.3
3-6-3	1.1
3-7-3	1.0
3-8-3	0.7
3-9-3	0.5
3-10-3	0.5
3-11-3	0.4

[a] The binding constants were calculated as the reciprocal of the 50% concentration of polyamine homologues required to displace 50% ethidium bromide bound to λ-DNA. The reproducibility with these results was within 3% in repeated measurements. The results are normalized with respect to spermine.

DISCUSSION

In this report, we present the results of a detailed study of the structural specificity effects of a series of spermine homologues on the condensation of λ-DNA. Although the main driving force behind DNA condensation is electrostatic in origin, our data demonstrate the important role played by polyamine structure in determining the midpoint concentrations and hydrodynamic radii of the condensates. The efficacy of spermine homologues in condensing DNA was in the following order: 3-6-3 < 3-5-3 ≈ 3-4-3 < 3-7-3 ≈ 3-8-3 < 3-9-3 < 3-10-3 ≈ 3-3-3 ≪ 3-2-3 ≈ 3-11-3 ≪ 3-12-3. Except for 3-2-3, which is not fully protonated at pH 7.4 (*41*), the lower homologues of spermine are more efficacious than the higher ones in condensing DNA. Schellman and Parthasarathy (*34*) used spermidine homologues differing in the number of methylene groups on one arm of the molecule to examine if interhelical separation conforms to physical models based on ligand structure and found that the Bragg spacings were a monotonically increasing function of the polyamine chain length. The spacings were intact, in accordance with a model in which amine groups make contact with phosphate groups on different DNA helices with bridging aliphatic chains fully extended. Although electrostatic interactions between the positive charges on the polyamines and the negative charges of DNA should be independent of ligand structure for isovalent cations, the remarkable structural effects observed with spermidine homologues by Schellman and Parthasarathy (*34*) and that reported herein with spermine homologues suggest that the ligand geometry might also play an important role in polyamine-mediated DNA compaction. The size of the DNA condensates (Table 1) increases with the length of the central methylene spacer between the secondary amino groups with $n > 6$. This may be due to the less compact nature of the individual DNA molecules in the presence of the higher homologues than the fully condensed form. This observation can also be related to the studies of Allison et al. (*32*), who noted that aggregation becomes more pronounced when spermidine is replaced by homologues having longer methylene bridges between the charges.

The polyamine homologue concentrations required for DNA condensation increased with increase in Na^+ concentration in the buffer. Theories based on electrostatic interaction of polyamines with DNA postulate ion competition, and hence the driving force for multivalent polyamine binding to DNA derives from a net gain in entropy by the release of DNA-bound Na^+ into solution:

$$\text{polyamine}^{4+} + \text{DNA}\cdot n\text{Na}^+ \rightarrow \text{DNA}\cdot(n-4)\text{Na}^+\cdot\text{polyamine}^{4+} + 4\text{Na}^+$$

When the bulk Na^+ concentration is increased in the medium, the net gain in entropy on releasing the bound Na^+ to the solution decreases, and an increased concentration of polyamines is required to compete with Na^+ and collapse DNA. Above 1500 mM Na^+, DNA condensation does not occur even when the concentration of spermine is increased 6 orders of magnitude above that required for DNA condensation in 1 mM Na^+ (*42*).

The dependence of the EC_{50} value of polyamines on $[Na^+]$ is represented by a plot of log $[EC_{50}]$ against log $[Na^+]$, yielding a straight line with slope values ranging from 0.9 to 1.6, depending on the chemical structure of the spermine homologue. This relationship follows from the equations of the counterion condensation theory (*8, 20, 21*):

$$1 + \ln(1000\theta_1/c_1\upsilon_{p1}) = -2z_1\xi(1 - z_1\theta_1 - z_2\theta_2)\ln(1 - e^{-\kappa b}) \quad (5)$$

$$\ln(\theta_2/c_2) = \ln(\upsilon_{p2}/1000e) + (z_2/z_1)\ln(1000\theta_1 e/c_1\upsilon_{p1}) \quad (6)$$

where c_1 and c_2 are the concentrations of counterions of charges z_1 and z_2 contributing to fractional charge neutralization of θ_1 and θ_2 and occupying volumes υ_{p1} and υ_{p2}, respectively, when they are bound to DNA and κ is the Debye screening parameter. $\xi = q_p^2/\epsilon kTb$ where q_p is the charge of the proton, ϵ is the bulk dielectric constant, and b is the average linear charge spacing of the polyelectrolyte in the absence of any associated ions. In other words, the parameter ξ is given by the ratio between the Bjerrum length and the average axial charge spacing, that is, the contour length divided by the number of charge groups. For double-helical B-DNA, $\xi = 4.2$, while for the single-stranded DNA, $\xi = 1.8$. These values were calculated by Manning (*20*) and Record et al. (*21*), while Olson and Manning (*43*) provided a configurational interpretation of this result. κ is given by the equation:

$$\kappa = 3.29z^{1/2}c_1^{1/2}\ (\text{nm}^{-1}) \quad (7)$$

Using this value of κ in eq 1 and introducing the first term of eq 1 into eq 2, the following equation can be derived after rearrangement:

$$\ln c_2 = [\ln\theta_2 - \ln(\upsilon_{p2}/1000e) + 2z_2\xi(1 - r)\ln(3.29bz^{1/2})] + z_2\xi(1 - r)\ln c_1 \quad (8)$$

In eq 8, $r = z_1\theta_1 + z_2\theta_2$, and the approximation of $\kappa b \sim 1 - e^{-\kappa b}$ has been introduced in eq 1. The maximum extent of charge neutralization of DNA by a combination of Na^+ and spermine has been calculated to be ~91% (*8*). Substituting this value for r, the slope of a plot of ln c_2 against ln c_1 can be calculated to be 1.5 from eq 4. Our experimentally determined values of the slope are very close to this value for homologues with an even number of methylene groups between the secondary amino groups of spermine. However, with homologues with an odd number of methylene groups in the bridging region, the slope values are close to 1, suggesting that the value of r can be higher than 0.91. For example, a slope value of 1 indicates ~94% charge neutralization of DNA by counterions. A possible reason for the differential effects of odd- and even-numbered methylene bridging regions on the slope values of Figure 5 might be the involvement of steric factors in the interaction of polyamines with DNA.

DNA condensation is an example of the polymer−globule transition, and under appropriate conditions of polymer length and stiffness, it is a readily reversible process which is favored by the association of sufficiently condensing multivalent cations with DNA (*44*−*48*). They cause localized bending or distortion of DNA at a critical extent of charge neutralization which facilitates the formation of rods and toroid-like structures. In addition to decreasing the net charge on DNA, they also aid in decreasing the unfavorable DNA segment−segment interactions. Thermodynamic analysis of polymer condensation was given by Post and Zimm (*49*) based on the Flory−Huggins lattice theory of polymer solutions by including a third viral coefficient to take into account the high local concentration of polymer segments in the condensed state. Recently, two models, the spool model (*50*) and the constant loop model (*51*), have been proposed as to how the DNA is wound within the toroid. The ligands are believed to affect the rotational dynamics and in turn the hydrodynamic radius by fluctuating the interionic forces analogous to electrolyte friction, by altering the hydration layer or structure of DNA (*52, 53*). Electrolytic friction is dependent only on the valence of the counterions whereas alteration of the hydration layer or DNA structure is expected to be quite sensitive to cation type (*54*).

Studies by Böttcher et al. (*50*) for spermidine- and uranyl acetate-induced DNA condensation indicated the formation of a series of complex multimolecular condensates with parallel bundles of DNA. Studies by atomic force microscopy (*44*) revealed the presence of multiple well-defined structural intermediates such as flowers and disks which leads to well-defined end points, including toroids or rod-shaped DNA. The nature of the structural intermediates depends on the concentration and nature of the condensing agent. In the present study, we notice that the spermine homologues exert a differential effect on the condensation process, depending upon their geometrical structure. However, it is not clear at present whether all these homologues follow the same condensation pathways with identical structural intermediates. The changes in the hydrodynamic radii and a slightly broader histogram for the condensates formed in the presence of higher homologues may be due to the formation of structural intermediates or higher order structures.

Our results on the relative binding affinity of spermine homologues to DNA (Table 2) shed some light on the binding of polyamines with DNA. Several models have been proposed for spermine−DNA interactions, and all these were based on direct electrostatic interactions between positive charges on the polyamines and negative charges of DNA.

Polyamine binding to DNA seems to depend on the distance between the positive charges on the polyamine relative to the distance between the negative charges on DNA phosphates. The negative charges of DNA phosphates can vary between 3.4 and 7.1 Å, and molecular mechanics calculations predict folding of DNA strands over polyamines, thereby enhancing their interactions (*55*, *56*). Early investigations by Suwalsky and others (*57*−*59*) assumed that the trimethylene spacing of 4.9 Å is suitable to interact with the adjacent phosphate groups while the tetramethylene spacing of 6.14 Å is suitable to bridge the phosphate groups between different duplex strands. Raman spectroscopic measurements indicate that the phosphodioxy band at 791 cm^{-1} for double-stranded DNA shifts downward upon complexation with spermine, and the deviations are influenced both by polyamine size and by concentration (*56*). Increasing the N−N distance beyond 11.2 Å allows the molecule to interact with two reactive sites located on different strands, and the presence of flexible groups can enable them to wrap around the DNA molecule instead of being localized in the minor/major groove. Moreover, the presence of methylene groups aids in establishing hydrophobic contacts between polyamines and DNA bases. The effectiveness of polyamines in condensing DNA is reduced by the fraction that enters into interhelical interactions. Therefore, the threshold concentration of 3-7-3 to 3-12-3 required to induce the condensation of DNA increases with increase in chain length. Increase in the EC_{50} value of 3-2-3 compared to spermine at pH 7.2 might be due to its decreased cationicity. The pK_a values (10.7, 10.0, 8.5, and 5.8) of this molecule at pH 7 (*41*) indicate that it may be a triamine under the conditions of our experiment. When the pH of the solution was decreased, we found a decrease in the critical concentration of 3-2-3 (unpublished results).

Several reports indicate the docking of spermine in the major groove of DNA (*27*−*29*). Evidence for minor groove binding was also presented by Bancroft et al. (*60*) and by Schmid and Behr (*61*). Different binding modes of spermine to poly(dG-dC) as compared to A-T-containing polynucleotides were also reported (*62*). Spectroscopic data and interpretations are also not consistent. For example, Deng et al. (*24*) concluded from Raman spectroscopic investigation of polyamine−DNA complexes that polyamine-induced DNA condensation is driven by nonspecific electrostatic binding, whereas analysis of Raman spectra by Ruiz-Chica et al. (*56*) supported the existence of structural specificities in polyamine−DNA interactions.

In short, our studies demonstrate that the regiochemical distribution of positive charge along the polyamines plays a major role in the condensation of DNA. Varying the number of methylene spacings in the bridging region between the two secondary amino groups of spermine had a profound effect on the molecule's ability to provoke structural changes in DNA, leading to its condensation. This structural effect might be useful in designing nonviral delivery vehicles for the transport of oligonucleotides and plasmid DNA in living cells for gene therapy applications.

ACKNOWLEDGMENT

We express our sincere thanks to Mr. Dan Snyder of Protein Solutions, Inc. (Charlottesville, VA), for his help in performing the dynamic laser light scattering measurements for the diffusion coefficients and hydrodynamic radii of condensed DNA particles.

REFERENCES

1. Bloomfield, V. A. (1996) *Curr. Opin. Struct. Biol. 6*, 334−341.
2. Livolant, F., and Ledorestier, A. (1996) *Prog. Polym. Sci. 21*, 1115−1164.
3. Blessing, T., Remy, J. S., and Behr, J. P. (1998) *Proc. Natl. Acad. Sci. U.S.A. 95*, 1427−1431.
4. Xu, Y., Hui, S. W., Frederik, P., and Szoka, F. C., Jr. (1999) *Biophys. J. 77*, 341−353.
5. Luo, D., and Saltzman, W. M. (2000) *Nat. Biotechnol. 18*, 33−37.
6. Lerman, L. S. (1971) *Proc. Natl. Acad. Sci. U.S.A.* 68, 1886−1890.
7. Gosule, L. C., and Schellman, J. A. (1976) *Nature 259*, 333−335.
8. Wilson, R. W., and Bloomfield, V. A. (1979) *Biochemistry 18*, 2192−2196.
9. Widom, J., and Baldwin, R. L. (1983) *Biopolymers 6*, 1595−1620.
10. Thomas, T. J., and Bloomfield, V. A. (1983) *Biopolymers 22*, 1097−1106.
11. Ong, E. C., Snell, C., and Fasman, G. D. (1976) *Biochemistry 15*, 468−477.
12. Eickbush, T. H., and Mondrianakis, E. N. (1976) *Cell 13*, 295−306.
13. Trubetskoy, V. S., Loomis, A., Slattum, P. M., Hagstrom, J. E., Budker, V. G., and Wolff, J. A. (1999) *Bioconjugate Chem. 10*, 624−628.
14. Bloomfield, V. A. (1997) *Biopolymers 44*, 269−282.
15. Arscott, P. G., Li, A. Z., and Bloomfield, V. A. (1990) *Biopolymers 30*, 619−630.
16. Marx, K. A., and Ruben, G. C. (1983) *Nucleic Acids Res. 11*, 1839−1854.
17. Golan, R., Pietrasanta, L. I., Hsieh, W., and Hansma, H. G. (1999) *Biochemistry 38*, 14069−14076.
18. Chattoraj, D. K., Gosule, L. C., and Schellman, J. A. (1978) *J. Mol. Biol. 121*, 327−337.
19. Lin, Z., Wang, C., Feng, X., Liu, M., Li, J., and Bai, C. (1998) *Nucleic Acids Res. 26*, 3228−3234.
20. Manning, G. S. (1978) *Q. Rev. Biophys. 11*, 179−246.
21. Record, M. T., Jr., Anderson, C. F., and Lohman, T. M. (1978) *Q. Rev. Biophys. 11*, 103−178.
22. Braunlin, W. H., Strick, T. J., and Record, M. T., Jr. (1982) *Biopolymers 21*, 1301−1314.
23. Wemmer, D. E., Srivenugopal, K. S., Reid, B. R., and Morris, D. R. (1985) *J. Mol. Biol. 185*, 457−459.
24. Deng, H., Bloomfield, V. A., Benevides, J. M., and Thomas, G. J., Jr. (2000) *Nucleic Acids Res. 28*, 3379−3385.
25. Dickerson, R. E., and Drew, H. R. (1981) *J. Mol. Biol. 149*, 761−786.
26. Jain, S., Zon, G., and Sundaralingam, M. (1989) *Biochemistry 28*, 2360−2364.
27. Gessner, R. V., Frederick, C. A., Quigley, G. J., Rich, A., and Wang, H.-J. (1989) *J. Biol. Chem. 264*, 7921−7935.
28. Tari, L. W., and Secco, A. S. (1995) *Nucleic Acids Res. 23*, 2065−2073.
29. Feuerstein, B. G., Pattabhiraman, N., and Marton, L. J. (1986) *Proc. Natl. Acad. Sci. U.S.A. 83*, 5948−5952.
30. Thomas, T. J., and Messner, R. P. (1988) *J. Mol. Biol. 201*, 463−467.
31. Thomas, T., and Thomas, T. J. (1993) *Biochemistry 32*, 14068−14074.
32. Allison, S. A., Herr, J. C., and Schurr, J. M. (1981) *Biopolymers 20*, 469−488.
33. Srivenugopal, K. S., Wemmer, D. E., and Morris, D. R. (1987) *Nucleic Acids Res. 15*, 2563−2580.
34. Schellman, J. A., and Parthasarathy, N. J. (1984) *J. Mol. Biol. 175*, 313−329.

35. Saminathan, M., Antony, T., Shirahata, A., Sigal, L. H., Thomas, T., and Thomas, T. J. (1999) *Biochemistry 38*, 3821−3830.
36. He, Y., Suzuki, T., Kashiwagi, K., Kusuma-Eguchi, K., Shirahata, A., and Igarashi, K. (1994) *Eur. J. Biochem. 221*, 391−398.
37. Igarashi, K., Koga, K., He, Y., Shimogori, T., Ekimoto, H., Kashiwagi, K., and Shirahata, A. (1995) *Cancer Res. 55*, 2615−2619.
38. Bloomfield, V. A. (1981) *Annu. Rev. Biophys. Bioeng. 10*, 421−450.
39. Morgan, A. R., Lee, J. S., Pulleyblank, D. E., Murray, N. L., and Evans, D. H. (1979) *Nucleic Acids Res. 7*, 547−569.
40. Antony, T., Thomas, T., Shirahata, A., and Thomas, T. J. (1999) *Biochemistry 38*, 10775−10784.
41. Stewart, K. D., and Gray, T. A.(1992) *J. Phys. Org. Chem. 5*, 461−466.
42. Widom, J., and Baldwin, R. L. (1980) *J. Mol. Biol. 144*, 431−453.
43. Olson, W. K., and Manning, G. S. (1976) *Biopolymers 15*, 2391−2405.
44. Fang, Y., and Hoh, J. E. (1998) *J. Am. Chem. Soc. 35*, 8903−8909.
45. Shen, M. R., Downing, K. H., Balhorn, R., and Hud, N. V. (2000) *J. Am. Chem. Soc. 122*, 4833−4834.
46. Yen, W. S., Rhee, K. W., and Ware, B. R. (1983) *J. Phys. Chem. 87*, 2148−2152.
47. Koltover, I., Wagner, K., and Safinya, C. R. (2000) *Proc. Natl. Acad. Sci. U.S.A. 97*, 14046−14051.
48. Lai, E., and Van Zenten, J. H. (2001) *Biophys. J. 80*, 864−873.
49. Post, C. B., and Zimm, B. H. (1979) *Biopolymers 18*, 1487−1501.
50. Böttcher, C., Endiskh, C., Furhop, J. H., Catterall, C., and Eaton, M. (1998) *J. Am. Chem. Soc. 120*, 12−17.
51. Hud, N. V., Downing, K. H., and Balhorn, R. (1995) *Proc. Natl. Acad. Sci. U.S.A. 92*, 3581−3585.
52. Schurr, J. M. (1980) *Chem. Phys. 45*, 119−132.
53. Schurr, J. M., and Schmitz, K. S. (1986) *Annu. Rev. Phys. Chem. 37*, 271−305.
54. Fujimoto, B. S., Miller, J. M., Ribeiro, N. S., and Schurr, J. M. (1994) *Biophys. J.*, 304−308.
55. Thomas, T. J., and Bloomfield, V. A. (1984) *Biopolymers 23*, 1295−306.
56. Ruiz-Chica, Medina, M. A., Sanchez- Jimenez, F., and Ramirez, F. Z. (2001) *Biophys. J. 80*, 443−454.
57. Suwalsky, M., Traub, Shmueli, V., and Subirana, J. A. (1969) *J. Mol. Biol. 42*, 363−373.
58. Tsuboi, M. (1964) *Bull. Chem. Soc. Jpn. 37*, 1514−1522.
59. Liquori, A. M., Constantino, L., Crecenzi, V., Elia, B., Giglio, E., Puliti, R., Desanti, S. M., and Vitigliani, V. (1967) *J. Mol. Biol. 24*, 113−122.
60. Bancroft, D., Williams, L. D., Rich, A., and Egli, M. (1994) *Biochemistry 33*, 1073−1086.
61. Schmid, N., and Behr, J. P. (1991) *Biochemistry 30*, 4357−4361.
62. Marquet, R., and Houssier, C. 1988) *J. Biomol. Struct. Dyn. 6*, 235−245.

BI010993T